

Intense particulate pollution events observed with lidar over the Paris Megalopolis

Patrick Chazette¹, and Philippe Royer²

¹Laboratoire des Sciences du Climat et de l'Environnement, CEA-CNRS-UVSQ, 91191 Gif-sur-Yvette Cedex, France, patrick.chazette@lscce.ipsl.fr

²LEOSPHERE, 76 rue de Monceau, 75008 Paris, France, proyer@leosphere.fr

ABSTRACT

The great particulate pollution event that affected the Paris Megalopolis in March 2014 was due to long-range transport from the northern-northeastern Europe. Although this phenomenon has appeared as exceptional in the media, this is not an exception and similar events have already been observed by lidar measurements. Here we will briefly describe and illustrate the origin of this intense pollution obviously harmful to health.

1. INTRODUCTION

Major aerosol pollution events may occur at the beginning of spring in the Paris Megalopolis, and even more throughout the northern part of France. We sampled four of these events from lidar systems located in the south of Paris. These measurements are one-off in space and time as they generally correspond to the opportunities offered during the preparation of large experimental campaigns as the Hydrological cycle in the Mediterranean eXperiment (HyMeX) [1].

We have already conducted several research projects on pollution aerosols in Paris Megalopolis using the lidar observations [2][3]. Lidar measurements were performed from ground-based station (fix or mobile) but also from airborne facilities [4]. This new study is based on lidar measurements acquired at different times since 2010 and recently during the particle pollution event of March 2014. We will not be exhaustive here, but we will mainly illustrate our work by the no less important pollution event occurring from 21 to 25 March 2011.

2. EXPERIMENTAL SET-UP

In all cases, two lidar have been used, the first one for aerosol optical properties and the second one for the wind intensity and direction. They were located ~30 km South of Paris (~48°42' N, 2°10' W). They worked during several days for sampling the major aerosol pollution event of April 2010, March 2011 (2 events) and March 2014. The Rayleigh-Mie lidar was similar to

the ALS450® lidar commercialized by Leosphere Company. The wind-lidar WindCube WLS70 is also a commercial Doppler coherent wind lidar developed and manufactured by Leosphere for meteorological applications. The main characteristics of the lidar are given in Table 1.

Table 1. Main characteristics of ground-based aerosol (ALS 450) and wind (WLS 70) lidars.

	ALS 450	WLS 70
Laser	Nd:YAG, flash-pumped, Q-switched Quantel Ultra	Master Oscillator + Erbium Doped Fiber Amplifier
Pulse length	5 ns	400 ns
Energy	16 mJ	50 µJ
Frequency	20 Hz	10 kHz
Reception channels	// 355 nm ⊥ 355 nm	1543 nm
Reception diameter	15 cm	10 cm
Field-of-view	~ 4 mrad	collimated
Detector	Photomultiplier tubes	Avalanche photodiode
Filter bandwidth	0.3 nm	-
Vertical sampling	15 m	50 m

3. GENERAL DESCRIPTION OF EVENTS

For the 4 major aerosol pollution events observed from our lidars, the origin is very similar. For instance, the situations as observed by MODIS are presented in Figure 1 for the events of 21-25 March 2011 and 12-15 March 2014. We have selected the most impacted days (23 and 14 March) where the pollution air mass advection is very well highlighted on the MODIS aerosol optical thickness (AOT) fields.

For these two cases, the aerosol plume is spread from East to West and advected from East. It traps particulate pollutants throughout its route passing over different aerosol sources that will be discussed hereafter. The

AOT at 550 nm is significantly larger than the mean value usually recorded throughout the year. In the aerosol plume it is larger than 0.3-0.4 on a large area compared with the background value of 0.15.

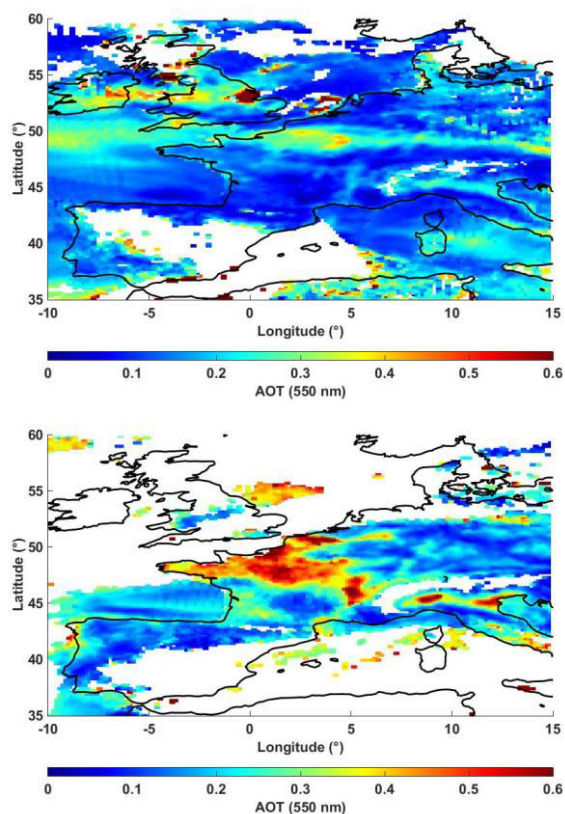


Figure 1. MODIS aerosol optical thickness (AOT) for 23 March 2011 (top panel) and 14 March 2014 (bottom panel).

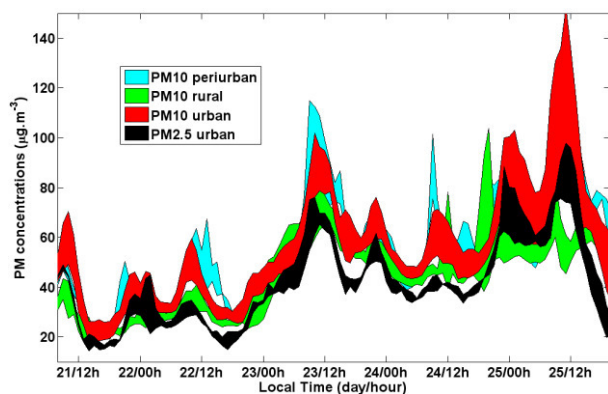


Figure 2. Example of temporal evolution of PM10 and PM2.5 concentrations observed by ground-based AIRPARIF network between 21 and 25 March 2011.

For the entire ground-based air quality network stations of AIRPARIF (<http://www.airparif.asso.fr/>) the mass concentrations of both PM2.5 and PM10 (Figure 2) significantly increased during all the considered events

(PM_x = mass concentration of particle with aerodynamic diameter less than x µm). The levels of particulate pollution are similar with PM10 reaching values larger than 100 µg m⁻³, which is twice the health tolerance required for outside air.

4. OVERLAP FUNCTION

For such pollution studies, the Rayleigh-Mie lidar must have an overlap function close to 1 at the lowest possible altitude. This is because the aerosol pollutants are mainly trapped in the planetary boundary layer (PBL) and the lower free troposphere (LFT). The overlap function is given in Figure 3. They are close to 1 at a distance of ~150 m from the emitter. A correction is possible for lidar data between 120 and 150 m. The lidar may be considered blind below 120 m.

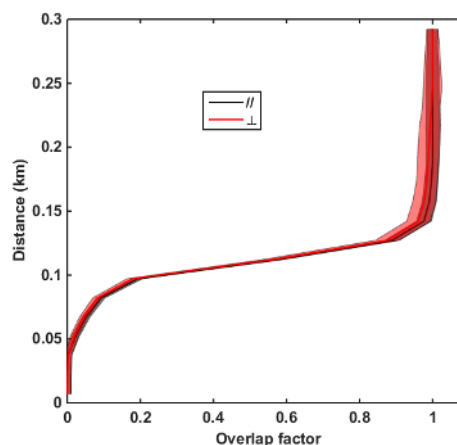


Figure 3. Overlap function of the Rayleigh-Mie lidar for the two polarization channels (parallel // and perpendicular ⊥).

5. EXAMPLE OF LIDAR MEASUREMENTS

As for the PM10 recorded at the ground level, the lidar shows a significant increase of the aerosol load in the PBL and LFT from 23 March 2011 (Figure 4). The AOT at 355 nm changes from ~0.2 to ~0.7. For the other aerosol pollution events we note similar AOT, sometime slightly higher (~0.9 for March 2014).

The inversion of lidar profile was performed using the sunphotometer as a reference during cloud-free daytime [2]. Hence, an equivalent backscatter to extinction ratio (inverse of the lidar ratio) has been retrieved, which can be compared with the sunphotometer-derived Angstrom exponent (Figure 5). The higher it is, the less the Angstrom is. In general, the larger aerosols are associated with the smaller Angstrom exponent. It may indeed be a contribution of terrigenous aerosols related

to the convection that develops during anticyclonic periods associated with these large particulate pollution events of early spring.

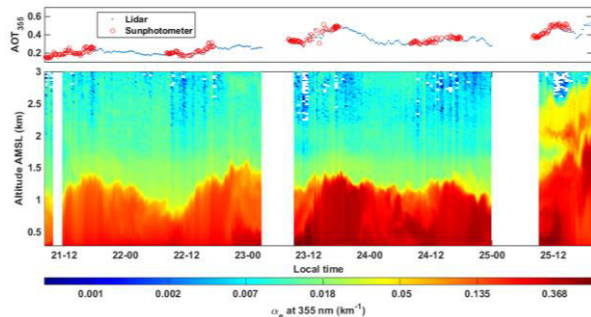


Figure 4. Time-height evolution of aerosol extinction coefficient at 355 nm (α_e) between 21 and 25 March 2011 (bottom panel). The aerosol optical thickness (AOT) is also given from the lidar (blue) and the sunphotometer (red) (top panel).

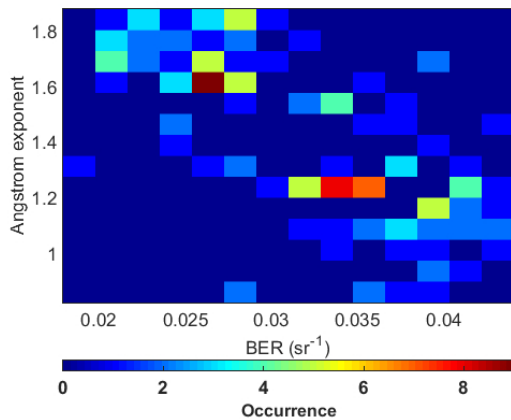


Figure 5. Angstrom exponent derived from the sunphotometer of the AERONET station of Palaiseau against the backscatter to extinction ratio (BER) from 21 to 25 March 2011.

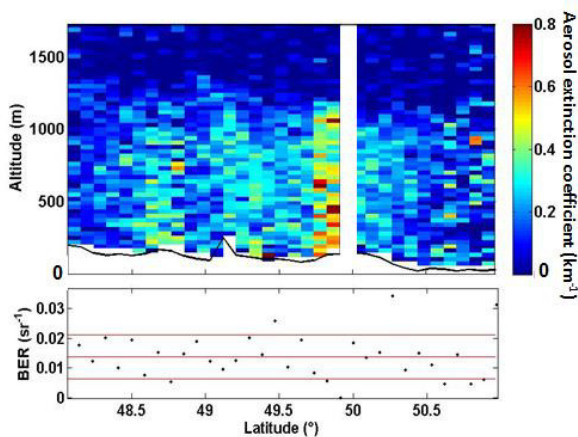


Figure 6. CALIOP-derived aerosol extinction coefficient and BER at 532 nm for 23 March 2011 1212 UTC.

We have also inverted the CALIOP profiles when the ground-track of the CALIPSO platform is close to Paris (Figure 6). The inversion was performed using MODIS-derived AOT as a reference [5]. Although the wavelengths are different (355 nm for the ground-based lidar and 532 nm for CALIOP), the comparisons between the BER seems not conclusive for the moment. In instance for the 23 March 2011, we found $0.029 \pm 0.005 \text{ sr}^{-1}$ and $0.013 \pm 0.005 \text{ sr}^{-1}$ at 532 and 355 nm, respectively. Note that the nearest CALIPSO orbit crosses the aerosol plume but this orbit is situated at 200 km east from Paris.

6. CONCLUSIVE DISCUSSION

The wind lidar very well highlights the origin of air masses crossing the Paris Megalopolis during the major aerosol pollution events. The two horizontal components of the wind are given in Figure 7 for the event of 21-25 March 2011. They are mainly recorder in the PBL due to the limited altitude range of the lidar. The aerosol plume is well established (Figure 1) with a horizontal wind from sector East between 3 and 7 ms^{-1} . After the 25 June, the wind veers and is from south-southwest below 1 km. This cannot sufficiently describe the air mass advection. Hence, we used backtrajectories computed from the Hysplit model (<http://www.arl.noaa.gov/HYSPLIT.php>).

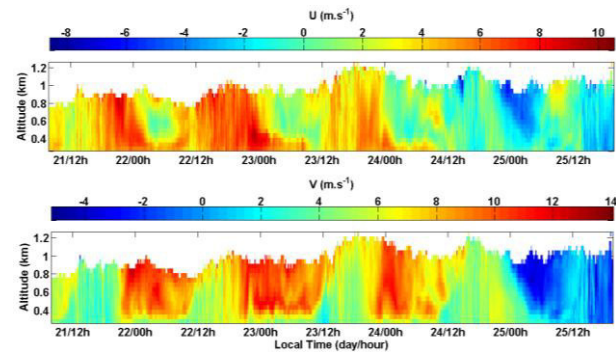


Figure 7. Temporal evolution of zonal (U, positive from North) and meridional (V, positive from east) wind derived from wind lidar (WLS70) between 21 and 25 March 2011.

The trajectories have been compared with the emission area of PM_{2.5} as defined from the EMEP data base (<http://www.emep.int/>). By this way, we can clearly check the origin of aerosol pollutants as shown Figure 8.

The events of high particulate pollution observed in France in March and April are the conditions of i) favorable weather to an east-west transport, ii) the

emissions of industrial areas of the Ruhr area and Benelux, and also iii) the use of fertilizers from animal droppings widely used in agriculture. The period from February to April is indeed favorable for mineralization of nitrogen in manure that is in the form of ammonia nitrogen. The fields thus become an important source of secondary aerosols that add to pollution from the East of France.

All these aerosols generally lead to a small particulate depolarization ratio ($PDR < 2\%$). In our cases study, this ratio is observed as higher and can be close to 10%, showing sometime the contribution of terrigenous particles from resuspension over dry soils. We have noted the dispersion in the PBL of dust-like aerosols is efficient during the afternoons with mean vertical speed velocity larger than 1 ms^{-1} .

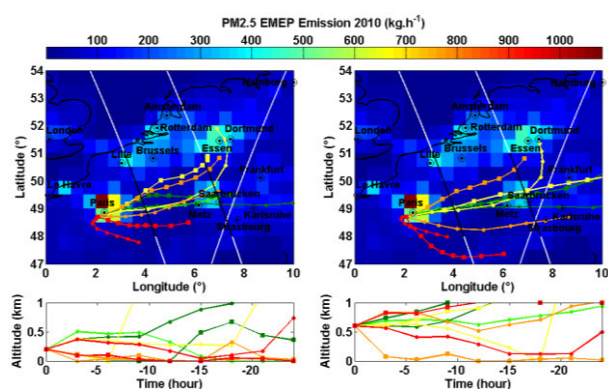


Figure 8. PM_{2.5} EMEP emission inventory for 2010 with a resolution of $0.5 \times 0.5^\circ$. One-day backward trajectory from Saclay starting at 200 m agl. (left column) and 800 m agl. (right column) for 21 (red), 22 (green), 23 (brown), 24 (black), 25 (yellow) March 2011 at 0h LT (squares) and 12h LT (circles). Available CALIOP orbits are indicated in white and the portion of the orbit considered is represented in black. Two daytime orbits are drawn for the 23 and 25 March, and one nighttime orbit for the 24 March.

This study has to be continued and the aerosol optical properties retrieved by the lidar measurements in terms of PDR and BER should be compared to those we met within London [6] and during the experiment conducted from Paris (France) to the lake Baikal (Russia) in 2013 [7].

ACKNOWLEDGMENTS

The MODIS and CALIOP data were obtained from the NASA Langley Research Center Atmospheric Science Data Center. The Hysplit model was used with the courtesy of NOAA Air Resources Laboratory (<http://www.arl.noaa.gov>).

REFERENCES

- [1] Chazette, P., F. Marnas, and J. Totems, 2014: The mobile Water vapor Aerosol Raman Lidar and its implication in the framework of the HyMeX and ChArMEX programs: application to a dust transport process, *Atmos. Meas. Tech.*, **7**, 1629-1647, doi:10.5194/amt-7-1629-2014.
- [2] Royer, P., Chazette, P., Sartelet, K., Zhang, Q. J., Beekmann, M., and Raut, J.-C., 2011: Lidar-derived PM₁₀ and comparison with regional modeling in the frame of the MEGAPOLI Paris summer campaign, *Atmos. Chem. Phys.*, **11**, 11861-11909, doi:10.5194/acp-11-11861-2011.
- [3] Raut J.-C. and P. Chazette, 2009: Assessment of vertically-resolved PM₁₀ from mobile lidar observations, *Atmos. Chem. Phys.*, **9**, 8617-8638.
- [4] Chazette P., H. Randriamiarisoa, J. Sanak, P. Couvert and C. Flamant, 2005: Optical properties of urban aerosol from airborne and ground-based in situ measurements performed during the ESQUIF program, *J. Geophys. Res.*, Vol. 110, No. D2, D0220610.1029/2004JD004810.
- [5] Royer, P., J.-C. Raut, G. Ajello, S. Berthier, and P. Chazette, 2010: Synergy between CALIOP and MODIS instruments for aerosol monitoring: application to the Po Valley. *Atmospheric Measurement Techniques* **3**, 1323-1359.
- [6] McMeeking, G. R., M. Bart, P. Chazette, J. M. Haywood, J. R. Hopkins, J. B. McQuaid, W. T. Morgan, J.-C. Raut, C. L. Ryder, N. Savage, K. Turnbull, and H. Coe, 2012: Airborne measurements of trace gases and aerosols over the London metropolitan region, *Atmos. Chem. Phys.*, **12**, 5163-5187, doi:10.5194/acp-12-5163-2012.
- [7] Dieudonné, E., P. Chazette, F. Marnas, J. Totems, and X. Shang, 2015: Lidar profiling of aerosol optical properties from Paris to Lake Baikal (Siberia), *Atmos. Chem. Phys.*, **15**, 5007-5026, doi:10.5194/acp-15-5007-2015.